Available online at www.sciencedirect.com

ScienceDirect

www.elsevier.com/locate/jes

JES JOURNAL OF ENVIRONMENTAL SCIENCES

www.jesc.ac.cn

Denitrification and microbial community in MBBR using *A. donax* as carbon source and biofilm carriers for reverse osmosis concentrate treatment

Li Li[1,2,3], *Guokai Yan*[1,2,3], *Haiyan Wang*[1,2,3,*], *Zhaosheng Chu*[1,3,4], *Zewen Li*[1,2,3], *Yu Ling*[1,2,3], *Tong Wu*[1,2,3]

1. *State Key Laboratory of Environmental Criteria And Risk Assessment, Chinese Research Academy of Environmental Sciences, Beijing 100012, China*
2. *Engineering Center for Environmental Pollution Control, Chinese Research Academy of Environmental Sciences, Beijing 100012, China*
3. *National Engineering Laboratory for Lake Pollution Control and Ecological Restoration, Chinese Research Academy of Environmental Sciences, Beijing 100012, China*
4. *State Environmental Protection Key Laboratory for Lake Pollution Control, Chinese Research Academy of Environmental Sciences, Beijing 100012, China*

ARTICLE INFO

Article history:
Received 2 March 2019
Revised 30 April 2019
Accepted 30 April 2019
Available online 10 May 2019

Keywords:
Arundo donax carbon source
Denitrification MBBR
Reverse osmosis concentrate
Nitrate removal
Microbial community
High-throughput sequencing

ABSTRACT

In this study, raw *Arundo donax* (*A. donax*) pieces were applied as carbon source and biofilm carriers for denitrification in a lab-scale moving bed biofilm reactor (MBBR) for the treatment of reverse osmosis concentrate gathered from local wastewater reuse plant. At stable phase (about 60 days), efficient denitrification performance was obtained with 73.2% ± 19.5% NO_3^--N average removal and 8.10 ± 3.45 g N/(m^3·day) NO_3^--N average volumetric removal rate. Mass balance analysis showed that 4.84 g *A. donax* was required to remove 1 g TN. Quantitative real-time PCR analysis results showed that the copy numbers of 16S r-RNA, *narG*, *nirS*, *nosZ* and anammox gene of carrier biofilm and suspended activated sludge in the declination phase (BF2 and AS2) were lower than those of samples in the stable phase (BF1 and AS1), and relatively higher copy numbers of *nirS* and *nirK* genes with lower abundance of *narG* and *nosZ* genes were observed. High-throughput sequencing analysis was conducted for BF2 and AS2, and similar dominant phyla and classes with different abundance were obtained. The class *Gammaproteobacteria* affiliated with the phylum *Proteobacteria* was the most dominant microbial community in both BF2 (52.6%) and AS2 (41.7%). The PICRUSt prediction results indicated that 33 predictive specific genes were related to denitrification process, and the relative abundance of 18 predictive specific genes in BF2 were higher than those in AS2.

© 2019 The Research Center for Eco-Environmental Sciences, Chinese Academy of Sciences. Published by Elsevier B.V.

* *Corresponding author. E-mail:* wanghy@craes.org.cn (Haiyan Wang).

https://doi.org/10.1016/j.jes.2019.04.030
1001-0742 © 2019 The Research Center for Eco-Environmental Sciences, Chinese Academy of Sciences. Published by Elsevier B.V.

Introduction

Moving bed biofilm reactor (MBBR) was established by AnoxKaldnes™ based on the combination of conventional activated sludge process and biofilm process in 1989 with the characteristics of bearing high treatment loading, small reactor space demand and high biomass (Odegaard et al., 1994). It has been proven that MBBR is an effective biotechnology for the treatment of nitrogen contaminated water through heterotrophic denitrification process (Kopec et al., 2018). The carrier material, structure and pore space configuration as well as the biofilm surface morphology affect the substrate transportation to the biofilm microbial community by influencing the flow velocity, and subsequently affect the nitrogen removal efficiency (Young et al., 2016). Polyethylene, polypropylene, polyurethane foams and haydite were commonly used in treatment of different kinds of nitrogen contaminated wastewater (Yuan et al., 2015). Composite-refined diatomaceous earth, polymeric nano-fibrous material, bioplastic based product, granular activated carbon, sand and home-made suspended ceramic product were also applied as carriers for nitrogen removal in MBBR systems (Dong et al., 2011). The application of novel economic carriers has been becoming the research focus for MBBR development (Dong et al., 2011).

Reverse osmosis (RO) technology is in incremental applications to produce high quality water from full scale municipal wastewater treatment plant (WWTP) effluent (Shannon et al., 2008). However, the RO concentrate (ROC) contains most contaminants and nutrients filtered out from the secondary effluents (Pradhan et al., 2016), whose genotoxicity and potential environmental risks are greatly increased (Umar et al., 2015). Cost-effective treatment methods for nitrogen removal from ROC is urgently needed to meet the nitrogen discharge standards and then reduce the environmental risks. Various technologies are applied for nitrogen removal from ROC, such as coagulation, UV/H_2O_2, ozonation, Fenton oxidation and biological processes (Umar et al., 2015). Nevertheless, few studies are carried out for the MBBR treatment of ROC.

Heterotrophic denitrification is the dominant biological process for nitrogen removal from ROC with nitrate (NO_3^--N) as the key nitrogen form (Umar et al., 2015), and its efficiency is affected by external carbon sources. Traditional liquid carbon sources such as ethanol, methanol, acetate and glucose are commonly used (Sun et al., 2017), and polyhydroxyalkanoates, polybutylene succinate and starch/polyvinyl alcohol polymer blends are reported both as solid carbon provider and biocarrier (Xu et al., 2018). Woodchip, corncob rice straw, retinervus luffae fructus and wheat straw (Yang et al., 2015) are also used as carbon sources. Bamboo charcoal and bamboo powder blended with other materials are applied as carbon source and biofilm carrier in denitrifying filters (Cao et al., 2016; Liu et al., 2018).

Arundo donax (*A. donax*) is widely distributed in fresh or moderately saline damp soils of mild temperate, subtropical and tropical regions, and the abundant cellulose and hemicellulose in its stalk could be easily degraded, thus makes it feasible to use raw *A. donax* pieces as carriers and carbon source for MBBR. Analysis of microbial community and its functions as well as gene copies are helpful to investigate the contaminant removal mechanism during biological processes. The microbial communities and gene copies are analyzed for various carriers and carbon sources in MBBR (Torresi et al., 2018). However, the differences of microbial communities and gene copies between the biofilm and the suspended sludge of MBBR are not studied, and the relationship of MBBR treatment efficiency and specific microorganism should be further illustrated.

In this study, raw *A. donax* pieces were used as carbon source and biofilm carriers in MBBR for the treatment of ROC gathered from the Dalton Filtration Reverse Osmosis (DFRO) unit of Beijing Cuihu Water Reuse Plant. DFRO is an advanced treatment unit for domestic wastewater reuse, which has lower operation pressure and cost compared with traditional reverse osmosis processes. The denitrification performance of *A. donax*-based MBBR was extensively explored, and mass balance was carried out. Furthermore, the denitrification gene copies and microbial communities in both biofilm and suspended activated sludge were analyzed and compared, and the correlations of specific bacteria functions and MBBR denitrification performance were also studied. Microbial community functions were predicted by PICRUSt based on high-throughput sequencing data.

1. Materials and methods

1.1. *A. donax* preparation and characterization

A. donax was harvested along Erhai littoral zone (25°36′–25°58′ N, 100°06′–100°18′ E) in July 2017. The aboveground parts of *A. donax* were cut into 2–3 cm pieces, then air-dried in the sun for 96 hr. When dried to relatively constant mass, the pieces were put into sealed bag and then reserved in dry and ventilated place.

Certain essential physical chemical parameters were measured to determine the compositions variation of *A. donax* and calculate the mass balance during the operation. *A. donax* pieces were cleaned and oven-dried at 40°C to constant mass, milled and screened through 60-mesh sieve, and then its cellulose, hemicellulose and lignin content were quantified using Van Soest's method (Hang et al., 2017). Total carbon (TC) and total nitrogen (TN) were determined by elemental analyzer (Thermo Flash 2000 CHNS/O, Thermo Fisher Scientific, USA), and total phosphorus (TP) was analyzed by Inductively Coupled Plasma Optical Emission Spectrograph (ICP-OES optima 8000, Perkin Elmer, USA). *A. donax* carriers were sampled before operation and after 170 days operation for compositions analysis.

1.2. Experimental set-up and operation design

1.2.1. Experimental set-up

Lab-scale plexiglas column with 12 L effective volume (25 cm in height and 25 cm in inner diameter) was set up as anoxic MBBR (Fig. 1). ROC was continuously supplied from the bottom of anoxic MBBR by peristaltic pump (BT100-1L, Baoding Lange Constant Pump Company, China) and then overflowed from

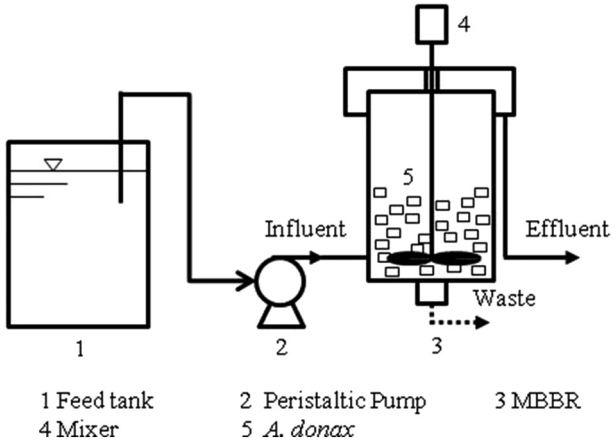

Fig. 1 – Schematic illustration of the experimental set-up.

the top with 12 hr hydraulic retention time (HRT). *A. donax* carriers were filled about 30% (*V/V*), and electric mechanical agitator was used to keep the suspension of carriers and sludge. Temperature in the bioreactor was controlled at 23–30°C by heating rods. The anoxic MBBR was covered by black shade to prevent photosynthesis disturbance. The experiments were carried out for 170 days, and the MBBR operation could be divided into three phases, i.e. inoculation phase (day 1–42), stable phase (day 43–98) and declination phase (day 99–170).

1.2.2. Sludge inoculation and operation design

The anoxic MBBR was inoculated by activated sludge taken from the anoxic tank of a municipal WWTP in Beijing, China. After inoculation, the mixed liquid suspended solids (MLSS), mixed liquor volatile suspended solids (MLVSS) and MLSS/MLVSS of the MBBR were 3544 mg/L, 1897 mg/L and 0.54, respectively.

The influent ROC of the anoxic MBBR was generated from the DFRO unit of a municipal WWTP in Beijing, China, which produces high quality reclaimed water. Certain amount of $NaNO_2$ and KH_2PO_4 were added in the influent ROC to keep nitrite (NO_2^--N) at about 10 mg/L (NO_2^--N loading rate of 0.2 g N/(m^2 carrier·day)) and the ratio of TN to TP was 20:1. The influent ROC ingredients for anoxic MBBR are shown in Table 1.

1.3. Microbial analysis

The *A. donax* carrier biofilm and active sludge samples were collected on the day 65 and day 170, all samples were prepared in triplicate. Before deoxyribonucleic acid (DNA) extraction, the biofilm on the carriers was detached using sterile brush and rinsed by ultrapure water (Elix, Millipore, USA), then allocated into 50 mL centrifuge tubes. The biofilm mixture or sludge was centrifuged at 3000 r/min for 20 min, and then stored at −20 °C after the removal of supernatant.

1.3.1. QPCR assay

Quantitative polymerase chain reaction (QPCR) assay was performed on ABI 7500 fast real time PCR platform (Life Technologies, USA) using SYBR-green based detection, which aimed to quantify the bacterial 16S r-RNA gene, *anammox* bacteria and the functional genes as *narG* (encoding NO_3^--N reductase), *nirK* (encoding cytochrome cd1 NO_2^--N reductase), *nirS* (encoding copper NO_2^--N reductase) and *nosZ* (encoding N_2O reductase). The primer sequences for target genes were shown in Table 2. The centrifuged biofilm (BF) and activated sludge (AS) samples of stable phase (BF1 and AS1) and declination phase (BF2 and AS2) were used for genomic DNA extraction by FastDNA® Spin Kit for Soil (MP Biomedicals, USA).

The 20 μL QPCR reaction mixture contained 16.4 μL 2X Taq Plus Master Mix (Vazyme Biotech, China), 2 μL template DNA, 0.8 μL forward primers and 0.8 μL reverse primers. QPCR was conducted under the following amplification procedure: pre-denaturation at 95°C for 5 min, melting 40 cycles of 5 sec at 95°C, annealing 40 cycles at different temperatures (60°C for 16S r-RNA gene, *narG* and *nirS*, 54°C for *nirK*, 56 °C for *nosZ* and 55 °C for *Anammox*) for 5 sec, and final extension at 72°C for 40 sec. Triplicate were run for all samples. The quantity and quality of the constructed plasmids were detected by Nano Drop 2000 analyzer (Thermo Fisher Scientific, USA). Plasmids were diluted to a series of 10-fold concentrations and used to obtain the standard curves. The R^2 values of standard curve

Table 1 – Characteristics of influent ROC.

Operation phases	Operation time (day)	pH	NO_3^--N (mg/L)	NO_2^--N (mg/L)	NH_4^+-N (mg/L)	COD (mg/L)	C/N ratio
Inoculation phase	1–42	6.8–7.7	3.7 ± 2.5	7.3 ± 4.5	1.1 ± 0.7	28 ± 13.8	1.9 ± 1.2
Stable phase	43–98	7.3–7.4	9.7 ± 2.7	6.5 ± 2.1	2.3 ± 0.8	26.7 ± 3.3	2.9 ± 0.3
Declination phase	99–170	7.0–8.0	13.2 ± 7.6	8.7 ± 8.5	1.3 ± 1.3	32.8 ± 25.4	1.4 ± 0.9

Table 2 – Primer sequences of target genes for QPCR.

Genes	Forward primers	Reverse primers	References
16Sr-RNA gene(Eub338/Eub518)	ACTCCTACGGGAGGCAGCAG	ATTACCGCGGCTGCTGG	Noah et al. (2005)
anammox (PLA46F/AMX667R)	GGATTAGGCATGAAGTC	ACCAGAAGTTCCACTCTC	Wouter et al., (2007)
nirK (876/1040)	ATYGGCGGVCAYGGCGA	GCCTCGATCAGRTTRTGGTT	Kim et al. (2011)
nirS (cd3af/R3cd)	GTSAACGTSAAGGARACSGG	GASTTCGGRTGSGTCTTGA	Satoshi et al. (2011)
nosZ (1527F/1773R)	CGCTGTTCHTCGACAGYCA	ATRTCGATCARCTGBTCGTT	Stres and Murovec (2009)
narG (1960m2f/2050m2r)	TA(CT)GT(GC)GGGCAGGA(AG)AAA	CGTAGAAGAAGCTGGTGCTGTT	Hang et al. (2017)

for bacterial 16S r-RNA gene, *anammox* bacteria and target genes ranged from 0.9949 to 0.9998, and the amplification efficiencies ranged from 84.8% to 97.3%.

1.3.2. High-throughput sequencing assay

Total genomic DNA of BF2 and AS2 was extracted using CTAB/SDS method. DNA concentration and purity were monitored on 1% agarose gels. DNA was diluted to 1 ng/μL using sterile water. 16S r-RNA genes of 16S V3-V4 were amplified used primers 515F (5′-GTGCCAGCMGCCGCGG-3′) and 806R (5′- GGACTACHVGGGTWTCTAAT-3′) with barcode. All PCR reactions were carried out by Phusion® High-Fidelity PCR Master Mix (New England Biolabs, USA).

The same volume of 1× loading buffer (SYB green contained) was mixed with PCR products, and then operated on 2% agarose gel for electrophoresis detection. Samples with bright main strip between 400 and 450 bp were selected for further experiments. PCR products were mixed in equidensity ratios. Then, mixture PCR products were purified by Qiagen Gel Extraction Kit (Qiagen, Germany). Following the manufacturer's recommendations and index codes, sequencing libraries were generated using TruSeq® DNA PCR-Free Sample Preparation Kit (Illumina, USA). The library quality was assessed by Qubit@2.0 Fluorometer (Thermo Fisher Scientific, USA) and Agilent Bioanalyzer 2100 system. At last, the library was sequenced on Illumina Hiseq2500 platform, and 250 bp paired-end reads were generated. The raw reads obtained from Illumina Hiseq2500 platform in this study were deposited in the NCBI sequence read archive under accession numbers SRR8607415 (sludge sample) and SRR8607416 (biofilm sample).

Paired-end reads were assigned to samples, and effective tags were obtained after filtering and chimera sequences removal using the QIIME (V1.7.0) quality controlled process and UCHIME algorithm. Sequences were assigned to the same operational taxonomic units (OTUs) at 97% identity, and Green Gene Database was used to annotate taxonomic information. Alpha diversity indices calculated by QIIME (Version 1.7.0) and displayed by R software (Version 2.15.3) were applied in the complexity analysis of species diversity. Alpha diversity indices were calculated according to reported formulas (Bing et al., 2016) and detailed in Appendix A.

1.3.3. PICRUSt prediction

Phylogenetic Investigation of Communities by Reconstruction of Unobserved States (PICRUSt) was used to predict the microbial community functions in the Kyoto Encyclopedia of Genes and Genomes (KEGG) database based on 16S r-RNA data (Langille et al., 2013). The closed reference OTU table based on the Green Gene Database was uploaded to the online PICRUSt prediction website (http://huttenhower.sph.harvard.edu/galaxy), and the K numbers corresponding to the molecular functions of individual genes and proteins, which were stored in KEGG Orthology (KO) database, were obtained and analyzed.

1.4. SEM and analytical method

In the stable period, the *A. donax* carriers were taken from reactor and cut into 5 mm × 5 mm pieces for attached biofilm morphology examination. The attached biofilm was immobilized by 2.5% neutral glutaraldehyde, washed by phosphoric acid buffer solution, dehydrated in increasing grades of ethanol, dried at critical point and then sprayed by gold before scanning electron microscope (SEM) observation.

Influent and effluent samples were collected every 3–4 days. Chemical oxygen demand (COD), ammonia (NH_4^+-N), TP, MLSS and MLVSS of sludge after inoculation were analyzed according to the standard methods (Sun et al., 2017). NO_2^--N and NO_3^--N were analyzed using ion chromatography (DIONEX ICS-1000, Dionex Inc., USA) after 0.45 μm syringe tip-filter filtration (SCAA-201). Dissolved oxygen (DO) and pH were measured by DO meter (LDO10103, HACH, USA) and pH meter (PHC10103, HACH, USA) using multi-parameters water analysis instrument (HQ-30d, HACH, USA).

1.5. Data analysis

The NO_3^--N removal efficiency and volumetric removal rate were calculated using the following equations:

$$NO_3^- \text{–}N \text{ removal efficiency} = \frac{C_{NO_3^-\text{–}N,\,inf} - C_{NO_3^-\text{–}N,eff}}{C_{NO_3^-\text{–}N,inf}} \times 100\%$$

$$NO_3^- \text{–}N \textit{ volumetic} \text{ removal rate} = \frac{\left(C_{NO_3^-\text{–}N,\,inf} - C_{NO_3^-\text{–}N,eff}\right) \times V}{V \times HRT} = \frac{\Delta C_{NO_3^-\text{–}N}}{HRT}$$

The C_{TIN} mentioned in this article was defined as follow:

$$C_{TIN} = C_{NO_3^-\text{–}N} + C_{NO_2^-\text{–}N} + C_{NH_4^+\text{–}N}$$

where, C_{TIN}, $C^+_{NH4\text{-}N}$, $C^-_{NO3\text{-}N,inf}$, and $C^-_{NO3\text{-}N,eff}$, are total inorganic nitrogen (TIN) concentration, NH_4^+-N concentration, influent and effluent NO_3^--N concentrations, respectively. V (L) is the effective volume of the anoxic MBBR.

The NO_2^--N and TIN removal efficiency and volumetric removal rate were calculated using similar equations.

2. Results and discussion

2.1. Characteristics of A. donax

2.1.1. Compositions change of A. donax

Two pieces of raw and used *A. donax* with similar shape and size were selected to measure the compositions (Table 3). Cellulose and hemicellulose degradation was reported as the carbon source for denitrification in constructed wetlands (Chen et al., 2011), so the cellulose (30.2%) and hemicellulose (32.2%) in the raw *A. donax* pieces could be hydrolyzed and degraded as the extra carbon source for denitrifying bacteria in denitrification MBBR. After 170 days operation, cellulose, hemicellulose, lignin, TN and TC contents per gram of *A. donax* were all reduced. It was worth noting that great sample weight loss of *A. donax* piece was observed. Based on the calculation of compositions and weight change of *A. donax* samples, it could be concluded that cellulose, hemicellulose, lignin, TC, and TN of raw *A. donax* pieces were reduced by 92.2%, 94.1%, 92.6%, 91.7% and 93.8% after 170 days operation. The hemicellulose decayed more than

Table 3 – Compositions variation of *A. donax*.

Group	Cellulose (g/g) [a]	Hemicellulose (g/g)	Lignin (g/g)	TC (g/g)	TN (g/g)	TP (g/g)	Sample weight (g/a piece)
Raw	0.37	0.32	0.20	0.48	0.01	4.3×10^{-4}	0.99
Used (after 170 days' operation)	0.34	0.22	0.18	0.47	7.1×10^{-3}	3.7×10^{-4}	0.08

[a] g/g means g/g *A. donax*.

cellulose, which was coherent with other report (Hang et al., 2017).

2.1.2. Surface properties

The surface properties as contact angle and surface structure were analyzed by pendent drop method and SEM (Fig. 2a, b). The outer surface of *A. donax* was hydrophobic with 117.5 ± 2.5° (n = 43) average contact angle, and it could be seen by SEM that the outer surface was smoother than the inner surface. The inner surface and sectional surface of *A. donax* pieces were rougher, thus more suitable for microbial attachment and biofilm formation than the outer surface. SEM pictures revealed that the relatively regular protrusion and void in the raw *A. donax* inner surface was conducive to the microbial attachment (Yang et al., 2015).

2.2. Denitrification performance

2.2.1. NO_3^-N removal

The *A. donax* MBBR reached stable phase (day 43–98) after 42 days inoculation, and NO_3^--N was removed effectively (Fig. 3a). Although the influent ROC quality fluctuated, the MBBR kept satisfactory denitrification performance with 73.2% ± 19.5% average NO_3^--N removal efficiency and 8.10 ± 3.45 g N/(m^3·day) average volumetric NO_3^--N removal rate. The results demonstrated that MBBR using *A. donax* pieces as carriers and carbon source for ROC treatment had relatively strong adaptability to the unstable ROC load, and the average effluent NO_3^--N kept at 1.82 ± 1.73 mg/L while the influent NO_3^--N was 5.87 ± 2.32 mg/L. After the stable phase, the NO_3^--N removal efficiency began to decline on day 108 and rapidly became negative, which might be caused by NO_2^--N oxidation as the dissolved oxygen (DO) in the reactor was 0.2 mg/L.

The average NO_3^--N removal efficiency and average volumetric NO_3^--N removal rate in this study was close to that of the similar systems. 18%–95% nitrogen removal efficiency was obtained for a bioreactor using woodchip as solid carbon source with 27.5 ± 4.5 mg influent NO_3-N/L and 7.2–51 hr HRTs, and the removal rate ranged from 8.0 to 18.0 g N-removed/(m^3·woodchips·day) (Christianson et al., 2017). Filamentous bamboo was also applied as supplemented carbon source for denitrification enhancement and good denitrification effect were obtained in these experiments (Chu and Wang, 2016).

2.2.2. NO_2^-N removal

Unlike the obvious variation of NO_3^--N removal efficiency in different phases, the *A. donax* MBBR maintained comparable high NO_2^--N removal efficiency during the whole operation (Fig. 3b). During the stable phase (day 43–98), the average NO_2^--N removal efficiency and volumetric removal rate were 84.1% ± 8.0% and 7.64 ± 4.03 g N/(m^3·day) under the condition of 4.4 ± 2.09 mg NO_2^--N/L influent. 83.4% ± 14.6% average NO_2^--N removal efficiency and 8.98 ± 5.36 g N/(m^3·day) average volumetric removal rate were obtained during the whole operation. The above-mentioned high NO_2^--N removal performance might be resulted from the anammox process, because DO in the reactor (0.2 mg/L) was suitable for the growth of anammox bacteria. Combined with 54.5% ± 30.7% average removal efficiency and 1.94 ± 2.3 g N/(m^3·day) volumetric

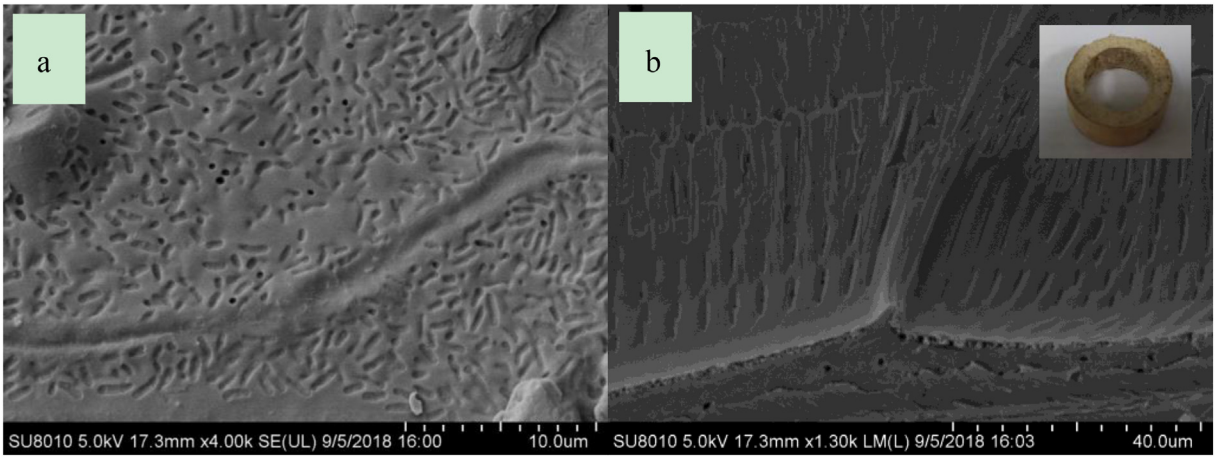

Fig. 2 – SEM micrographs of *A. donax* surface (a 4000×, b 1300×) and photo of *A. donax* piece (upper right corner of b) before biofilm inoculation.

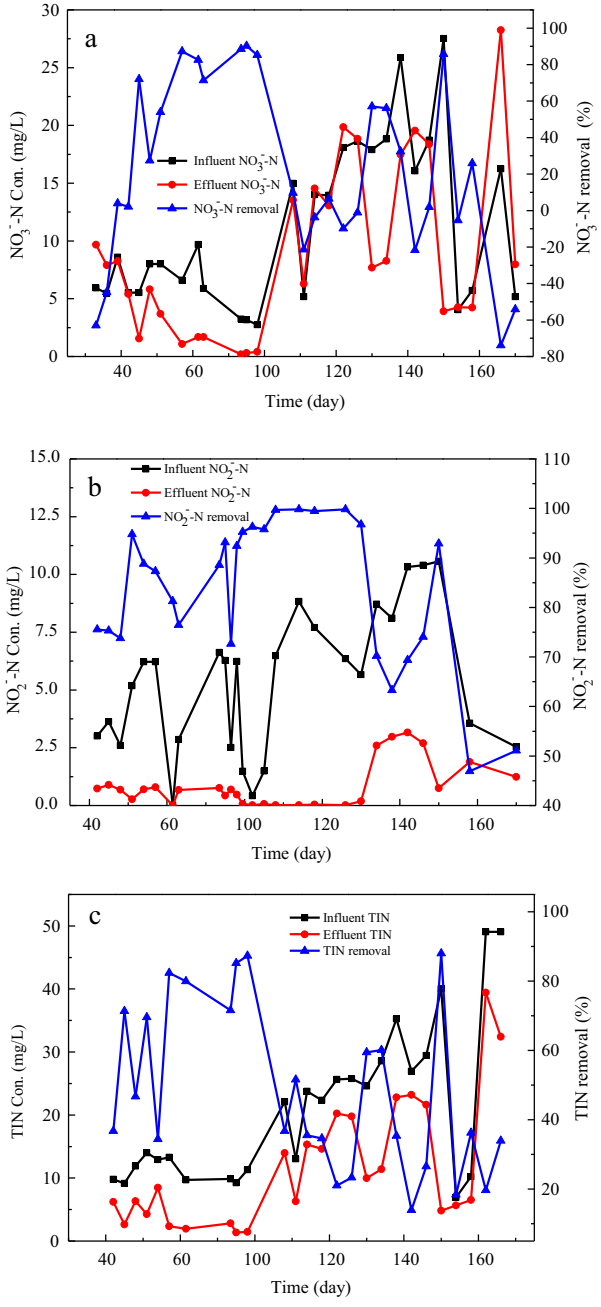

Fig. 3 – NO_3^--N (a), NO_2^--N (b) and TIN (c) removal efficiency of the *A. donax* MBBR.

removal rate of NH_4^+-N throughout the whole operation, the proportional NO_2^--N removal amount could be calculated according to the anammox reaction process (Eq. (1)).

$$NH_4^+ + 1.32NO_2^- + 0.066HCO_3^- + 0.13H^+ \rightarrow 1.02N_2 + 0.26NO_3^- + 0.066CH_2O_{0.5}N_{0.15} + 2.03H_2O \quad (1)$$

Though the NO_2^--N removal efficiency kept high throughout the whole experiment, slight variation could be observed. NO_2^--N removal efficiency increased to 94.8% on day 51, kept stable (91.7% ± 8.0%) for a long time (day 51–130), and then declined to 66.8% ± 14.2%. NO_2^- accumulation was occurred after 130 days operation, which was probably resulted from the depletion of *A. donax* endogenous carbon source. When NO_3^- removal was incomplete due to inadequate carbon source, NO_2^- would accumulate because of the different reduction rates of NO_2^- and NO_3^- reductase caused by electron donors' competition (Ge et al., 2012).

2.2.3. TIN removal

At stable phase, the removal efficiency and volumetric removal rate of TIN were 69.8% ± 17.0% and 15.5 ± 4.02 g N/(m^3·day) when the influent and effluent TIN were 11.26 ± 1.75 mg/L and 3.51 ± 2.29 mg/L, respectively (Fig. 3c). TIN removal efficiency began to decline on day 99, and the average TIN removal efficiency kept 31.1% ± 19.2% during declination phase, which might be owing to the NO_3^--N increase caused by influent fluctuation and *A. donax* carbon source depletion. However, the TIN volumetric removal rate, which was 14.54 ± 9.61 g N/(m^3·day) at declination phase, remained relatively steady until day 142. The anammox reaction between NO_2^--N and NH_4^+-N was the potential key factor for the above-mentioned phenomenon, which needs further investigation. Furthermore, the nitrogen release from *A. donax* would influence the TIN removal efficiency, which was concealed by the influent fluctuation.

2.2.4. NH_4^+-N and COD variation

The influent NH_4^+-N was low but fluctuated with an average value of 1.40 ± 1.17 mg/L, which was caused by the instability of DFRO unit and decomposition of organic nitrogen in *A. donax* (Fig. 4a). In the first 26 days, the influent NH_4^+-N was around 1.0 mg/L, then kept relatively high from day 27 to day 105 with the maximum value of 5.42 mg/L. Afterwards, the influent NH_4^+-N decreased to 1.0 mg/L again. The average NH_4^+-N removal efficiency and volumetric removal rate during the whole operation were 54.5% ± 31.2% and 1.94 ± 2.34 N/(m^3·d), which verified the existence of anammox reaction in the anoxic MBBR.

The effluent COD variation could be divided into two stages (Fig. 4b). In the first 13 days, the effluent COD averaged at 1441.0 ± 300.2 mg/L, then decreased gradually and kept at relatively stable level (20.2 ± 12.9 mg/L) from day 27. The rapid COD increase in the first 13 days was probably caused by the soluble organic matter release from *A. donax* carriers and the low carbon usage by the biofilm and sludge. Then much released carbon was consumed continuously by the matured biofilm and sludge, thus kept the COD at stable concentration. The results also indicated that the organic matter release rate from *A. donax* was high during the first 2 weeks and then began to decrease after that period. Other plant carbon source exhibited similar release trend with slight differences of rapid release time (Yang et al., 2015). Effluent COD before day 27 was high enough to cause secondary environmental pollution, which should be collected and partly recycled to the influent as external carbon source. Certain measures should be taken for the effluent before day 27 to meet the COD discharge limitation. Appropriate pretreatment, modification or combination with other materials of the plant carbon source could stabilize its carbon release (Liu et al., 2018), and such measures could also be applied to *A. donax* pieces for steady carbon release.

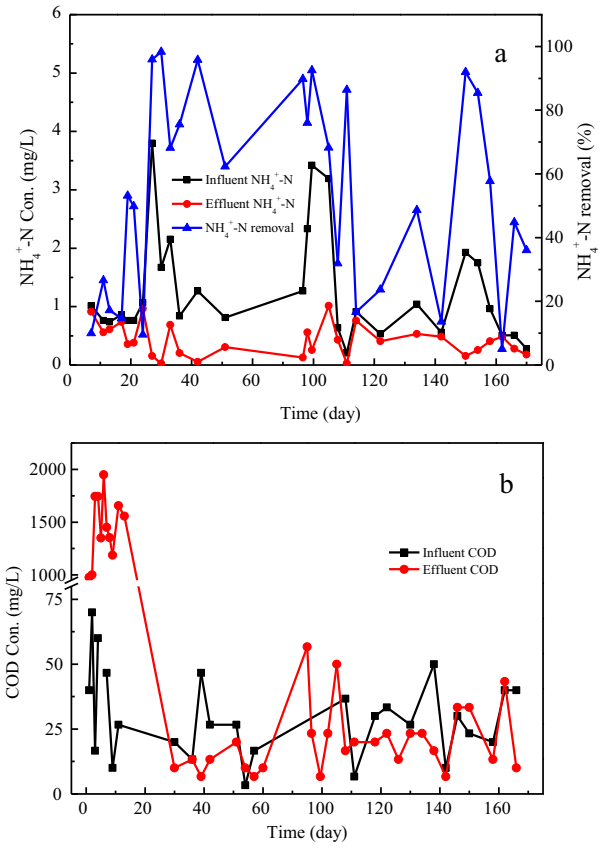

Fig. 4 – NH_4^+-N (a) and COD (b) variation in *A. donax* MBBR.

2.3. Mass balance calculation

Mass balance among nitrogen, carbon and *A. donax* was calculated after 170 days operation (Table 4). Influent and effluent TIN mass were calculated by the influent and effluent average TIN concentration multiplied by the operation days and daily wastewater treatment amounts. Influent and effluent total organic carbon (TOC) mass were obtained by similar method. TN (TC) mass released from *A. donax* carriers was generated from the weight and TN (TC) content of the raw and used *A. donax* in the MBBR reactor. TC and *A. donax* needed for 1 g nitrogen removal were calculated by the total removed TN mass as well as the total consumed TC and *A. donax* mass.

The calculation results indicated that 4.84 g *A. donax* was required for 1 g TN removal, which was similar to other studies, e.g., 4.72 g starch/polycaprolactone for a packed-bed denitrification bioreactor (Shen et al., 2013), 4.77 g corncob for a corncob carbon source and bamboo charcoal filter combined nitrogen removal system (Cao et al., 2016). In consideration of the carbon loss and carbon consumption for bacteria assimilative growth in practical applications, more *A. donax* should be dosed than the theoretical value.

2.4. Microbial community structure

2.4.1. SEM

At stable phase, the biofilm bacterial morphology on *A. donax* surface was observed by SEM (Fig. 5a, b). The surface of *A. donax* was covered by dense biofilm mainly consisted of cocci (0.5–2.0 μm), bacillus (0.5–1.0 ~ 1–5.0 μm) and filamentous bacteria, which was consistent with the microbial morphology in a packed-bed denitrification bioreactor using biodegradable polymer corncob as carbon source (Shen et al., 2013). Chu and Wang (2016) also reported that the filamentous, cocci and short rod bacteria were the main bacteria in three denitrification packed bed reactors, which were filled with PHBV, PHBV/starch and PHBV/bamboo powder (BP) blends as carbon source and biofilm carriers.

Table 4 – Mass balance of nitrogen and carbon for *A. donax* MBBR denitrification.

Item	Indexes	Mass (g)
Nitrogen		
In	Influent TIN	85.36
–	TN released from *A. donax*	4.08
Out	Effluent TIN	48.00
Removed	Total removed TN	41.44
Carbon		
In	Influent TOC[a]	70.30
–	TC released from *A. donax*	195.93
Out	Effluent TOC	170.13
Consumed	Total consumed TC	96.11
	Total consumed *A. donax*	200.66
Required/g N	TC	2.32
	A. donax	4.84

[a] : TOC was calculated from the liner relation with COD (R^2 = 0.83).

2.4.2. Gene abundance

The copy numbers of 16S r-RNA gene (BF1: 2.9×10^{10}/g·BF, AS1: 4.5×10^{10}/g·AS, BF2: 1.3×10^{10}/g·BF, AS2: 3.7×10^{9}/g·AS) and *narG* (BF1: 1.7×10^{7}/g·BF, AS1: 7.0×10^{6}/g·AS, BF2: 8.9×10^{6}/g·BF, AS2: 1.6×10^{6}/g·AS) in BF and AS of *A. donax* denitrification MBBR (Fig. 6) were similar with those of denitrifying MBBR (Torresi et al., 2018). and other plant–biomass carbon source denitrification systems (Arantzazu et al., 2011; Ji, 2018; Torresi et al., 2018). The copy numbers of *nirS* (BF1: 1.5×10^{10}/g·BF, AS1: 6.4×10^{9}/g·AS, BF2: 3.2×10^{9}/g·BF, AS2: 8.1×10^{8}/g·AS) and *nirK* (BF1: 2.2×10^{8}/g·BF, AS1: 2.5×10^{8}/g·AS, BF2: 2.3×10^{8}/g·BF, AS2: 4.5×10^{7}/g·AS) were in the same order of magnitude with those in wetland nitrogen removal system (Arantzazu et al., 2011), but the numbers of *nosZ* were lower than those reported in similar woodchip denitrification bioreactors (Ji, 2018). In this study, the copy numbers of *nosZ* (BF1: 3.0×10^{6}/g·BF, AS1: 1.7×10^{6}/g·AS, BF2: 8.7×10^{4}/g·BF, AS2: 4.3×10^{4}/g·AS) genes were 1 to 6 orders of magnitude lower than those of *nirS* and *nirK*, which indicated that possible N_2O accumulation occurred because the majority of NO_2^--N reduced to N_2O by *nirS* and *nirK* could not be reduced completely without enough *nosZ* genes. The copies of *nirS* were up to 10 times higher than those of *nirK* in both BF and AS, which was consistent with previous studies about biological nitrogen removal ecosystems (Torresi et al., 2018), and such phenomenon might be caused by the stricter anaerobic environment requirement of *nirK* than *nirS* gene (Wei and Ji, 2014).

The *nirK* gene was almost unchanged in the BF samples of stable and declination phases, but the copy numbers of 16S r-

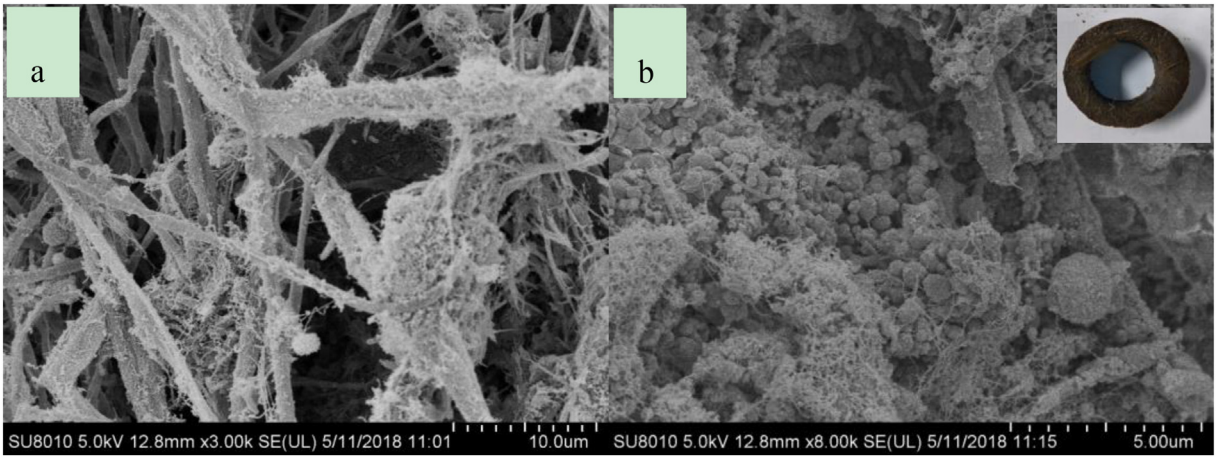

Fig. 5 – SEM micrographs of *A. donax* surface (a 3000×, b 8000×) and photo of *A. donax* piece (upper right corner of b) after biofilm inoculation.

RNA gene, *narG*, *nirS* and *nosZ* in BF2 were 55.2%, 47.8%, 79.3%, 97.1% and 99.7% less than those in BF1, respectively. Compared with AS1, the copy numbers of 16S r-RNA gene, *narG*, *nirK*, *nirS* and *nosZ* in AS2 decreased 91.7%, 77.7%, 82.5%, 87.4% and 97.4%, respectively. The decrease of all the above-mentioned genes in BF samples was lower than those in AS samples, which suggested that the biofilm microorganisms had higher resistance to unfavorable conditions to some extent.

The total copy numbers of denitrification genes (*narG*, *nirK*, *nirS* and *nosZ*) in BF1, BF2, AS1 and AS2 were 1.6×10^{10} copies/g·BF, 3.4×10^{9} copies/g·BF, 6.7×10^{9} copies/g·AS and 8.5×10^{8} copies/g·AS, respectively. Both the copy numbers of denitrification genes in BF were higher than those in AS at two phases, which meant higher denitrifying microbial richness in BF than AS. When the MBBR was approaching the declination phase, the copy numbers of denitrification genes were decreased because of the insufficient carbon source.

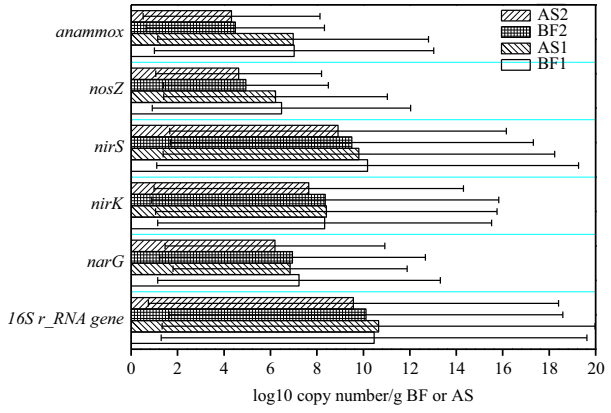

Fig. 6 – Copy numbers of the bacterial 16S r-RNA, narG, nirS, nirK, nosZ and anammox genes in BF and AS of *A. donax* MBBR.

The copy numbers of *Anammox* gene in BF1, BF2, AS1 and AS2 were 1.0×10^{7} copies/g·BF, 3.1×10^{4} copies/g·BF, 9.5×10^{6} copies/g·AS and 2.1×10^{4} copies/g·AS, respectively, which suggested the existence of *anammox* reaction and thus explain the phenomenon of Sections 2.2.2–2.2.4. The copy numbers of *nirS* and *nirK* were 1 to 3 orders of magnitude higher than those of *narG* in both BF and AS, which was probably caused by the relatively high influent NO_2^--N (7.3 ± 4.5 mg/L) during inoculation phase.

2.4.3. Microbial community diversity

High-throughput sequencing assay was used to study the microbial diversity of BF2 and AS2 (the NCBI accession numbers of SRR8607415 for AS and SRR8607416 for BF). After low quality sequences and chimeras removal, 93,434 and 90,079 effective sequences were selected for further analysis in BF2 and AS2. The effective tags of BF2 and AS2 samples were clustered (with ≥97% similarity) into1816 and 2260 OTUs.

Alpha diversity indexes of the microbial community variation of BF2 and AS2 were listed in Table 5. The coverage indexes of BF2 and AS2 were 0.995 and 0.994, which were high enough to ensure the remarkable representativeness of the identified sequences for the majority of microbial diversity (Matar et al., 2017). ACE, Chao 1 and Shannon values (2487.4, 2455.5 and 8.2) of AS2 were higher than those (2034.1, 1975.6 and 7.8) of BF2, which indicated the relatively higher microbial diversity in AS2 than that in BF2 as reported by Bing et al.

Table 5 – Alpha diversity analysis for BF2 and AS2 samples.

Sample	OTUs	Shannon	ACE	Chao 1	Coverage	Simpson
BF2	1816	7.78	2034.13	1975.61	0.995	0.016
AS2	2260	8.24	2487.36	2455.48	0.994	0.016

(2016). AS2 and BF2 had the same Simpson values, which meant similar microbial evenness. It was reported that multi-stage MBBR had higher microbial richness than single-stage MBBR (Torresi et al., 2018), which was consistent with the lower alpha diversity indexes of single-stage *A. donax* MBBR in this study. The results of 16S r-RNA high-throughput sequencing suggested that there was minor difference of dominant groups between BF2 and AS2 (Fig. 7a). There were the same dominant phyla of *Proteobacteria* (64.3% and 50.1%), *Bacteroidetes* (7.9% and 5.5%), *Firmicutes* (7.6% and 12.1%), *Chloroflexi* (5.6% and 3.5%), *Acidobacteria* (4.4% and 3.7%) and *Gemmatimonadetes* (1.4% and 10.4%) with different amount in BF2 and AS2, however, the *Actinobacteria* (4.4%) only existed in BF and *Planctomycetes* (4.9%) only in AS. Obviously, *Proteobacteria* were the main dominant community in both BF (64.31%) and AS (50.1%), which were in accordance with the previous reports, e.g., 37%–89% (Biswas et al., 2014) and 85.5% (Shen et al., 2013) for different scale denitrification systems. *Proteobacteria* community were Gram-negative bacteria and contained large number of denitrificans (Bing et al., 2016), whose outer surface lipopolysaccharides could assist their attachment to the carrier surface (Biswas et al., 2014). *Bacteroidetes* and *Firmicutes* were found as dominant phyla in two full-scale MBBRs with suspended polyethylene carriers and other lab-scale denitrification reactors, and many strains of *Bacteroidetes* and *Firmicutes* had been identified as denitrifcans (Biswas et al., 2014; Shen et al., 2013; Xu et al., 2018). The same predominant bacterial classes in BF and AS were *Gammaproteobacteria* (52.6%, 41.7%), *Clostridia* (5.6%, 6.4%), *Anaerolineae* (5.3%, 3.0%), *Bacteroidia* (4.8%, 3.4%), *Deltaproteobacteria* (3.3%, 3.9%) and *Bacilli* (1.6%, 4.9%) (Fig. 7b). However, the other dominant classes of *Alphaproteobacteria* (8.3%), *unidentified_Actinobacteria* (3.8%) and *Deltaproteobacteria* (3.3%) were only found in BF, and *unidentified_Gemmatimonadetes* (10.4%) and *Planctomycetacia* (3.5%) were only observed in AS. *Gammaproteobacteria*, *Alphaproteobacteria*, *Deltaproteobacteria* and *Clostridia* were also found as the dominant denitrification groups in other denitrification systems (Biswas et al., 2014; Bing et al., 2016). Types of carbon source, the availability of organic substrate and the stages of MBBR could influence the microbial communities of biofilm and suspended sludge (Torresi et al., 2018).

At genus level, the bacterial sequences in BF mainly belonged to *Acinetobacter* (10.9%), *Denitratisoma* (2.9%) and *Pseudomonas* (2.8%). However, *Lactobacillus* (4.4%), *Denitratisoma* (3.1%) and *Sulfuritalea* (2.2%) were the dominant genera in AS. There were the same genera of *Denitratisoma* and *Acinetobacter* with different abundance in BF and AS, and other genera were different (Fig. 7c). *Acinetobacter*, which belonged to *Gammaproteobacteria* class, were the predominant bacteria in both biofilm and suspended sludge from MBBR (Biswas et al., 2014). *Pseudomonas* contained typical denitrification bacteria which participated in denitrification, nitrogen fixation and carbon degradation process, and were dominated in anoxic denitrification biofilm reactor (Bing et al., 2016). Fig. 7c suggested that *Pseudomonas* in BF were more abundant than those in AS, which might be resulted from higher consumption of *A. donax* released carbon source by *Pseudomonas* in BF than those in AS for the shorter transportation distance. Moreover, the stronger anoxic environmental condition in the BF inner surface of

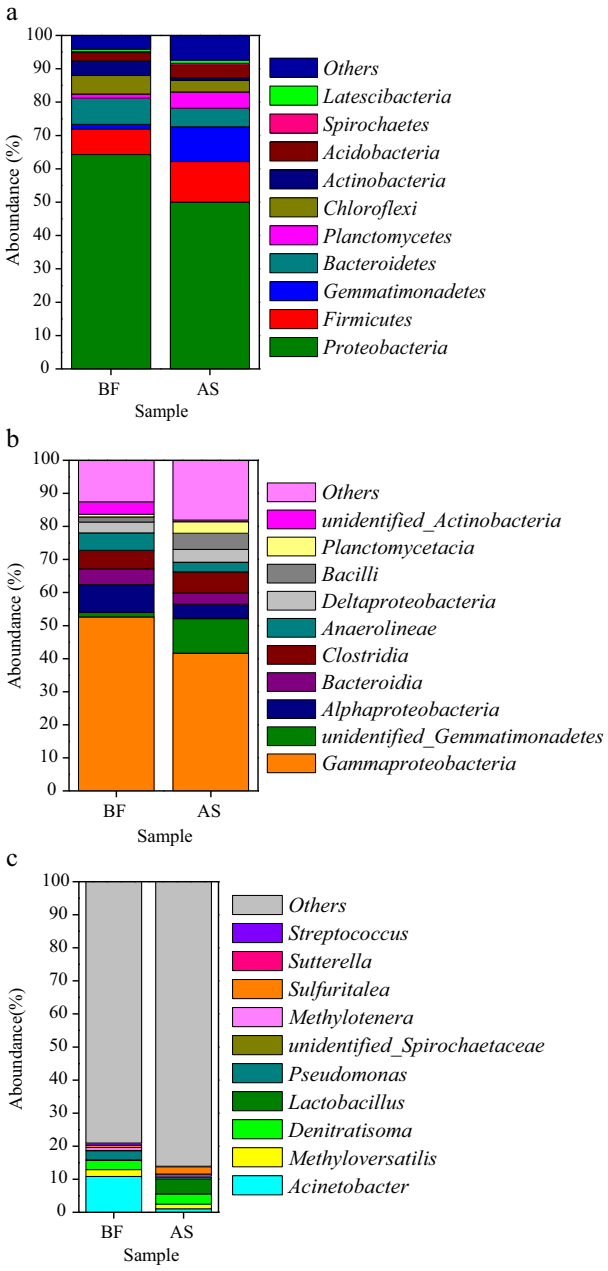

Fig. 7 – Microbial community diversity and its composition in BF and AS at Phylum level (a), Class level (b) and Genus level (c).

A. donax was relatively favorable for *Pseudomonas* growth. *Lactobacillus* were related to NO synthesis (Yarullina and Ilinskaya, 2007). *Denitratisoma* were typical heterotrophic bacteria affiliated with *Proteobacteria* phylum, which were detected in wastewater denitrification system (Zhang et al., 2017).

2.4.4. Functional prediction of microbial community

PICRUSt results illustrated that the Nearest Sequenced Taxon Index of BF2 and AS2 were 0.11 and 0.16 respectively, which were similar with those reported by Li et al. (2017). The K

number in BF (5716) was lower than that in AS (6019), which was corresponded with the lower OTU numbers of BF2 than AS2 in Section 2.4.3. For both BF2 and AS2, the predicted functions can be classified into 6 categories at KO level 1, 41 categories at KO level 2, and 295 (BF2) and 297 (AS2) categories at KO level 3. The most abundant functions at KO level 1, level 2 and level 3 were metabolism, membrane transport and transporters, respectively.

There were 33 predictive specific genes related to denitrification process in the prediction results, which included 21 genes about NO_3^--N/NO_2^--N reduction, 11 genes about NO reduction and 1 gene about N_2O reduction (Appendix A Table S1). The predictive denitrification functional genes included NO_3^--N/NO_2^--N reductase, NO_3^--N/NO_2^--N transporter, NO_3^--N/NO_2^--N response regulator, NO_3^--N/NO_2^--N sensor histidine kinase, NO reductase, NO dioxygenase, NO sensitive transcriptional repressor, N_2O reductase, etc. The total abundance of predictive denitrification functional genes and the relative abundance of 18 predictive specific genes in BF2 were higher than those in AS2, which suggested the higher denitrification capacity of BF2 than AS2. Moreover, the relative lower abundance of N_2O reductase and higher abundance of NO reductase illustrated the accumulation of N_2O in the *A. donax* denitrification MBBR. However, the prediction of denitrification was limited as the annotated anammox process is insufficient in KEGG database (Li et al., 2017).

3. Conclusions

Raw *A. donax* pieces could be used as carbon source and biofilm support to remove NO_3^--N from ROC in a denitrification MBBR, the feasibility and microbial community characteristics of which were extensively investigated and demonstrated in this study. High denitrification capability (73.2% ± 19.5% NO_3^--N removal efficiency and 8.10 ± 3.45 g N/(m^3·day) NO_3^--N volumetric removal rate) were obtained at stable phase (60 days). The NH_4^+-N removal efficiency of 54.5% ± 31.2% was achieved due to the anammox process, which had been verified by the QPCR analysis. COD release from *A. donax* pieces was excessive in the first 13 days, which kept at relatively stable level from day 27.

All of the copy numbers of 16S r-RNA, *narG*, *nirS*, *nosZ*, and anammox genes in declination phase (BF2, AS2) were lower than those in stable phase (BF1, AS1). The copy numbers of *nirK* in BF1 and BF2 were closed, and the copy number of *nirK* in AS1 was higher than that in AS2. The copy numbers of *narG*, *nirS*、*nosZ* and anammox genes in BF were higher than those in AS, and the abundance of *nirS* and *nirK* genes were higher than that of *narG* and *nosZ* genes for both BF and AS. However, the microbial diversity of BF2 was relatively lower than that of AS2. Similar dominant phyla and classes with different abundance were obtained for BF2 and AS2. There were the same dominant phyla of *Proteobacteria* (64.3% in BF2 and 50.1% in AS2), *Bacteroidetes* (7.9% in BF2 and 5.5% in AS2) and *Firmicutes* (7.6% in BF2 and 12.1% in AS2), etc. The classes of *Gammaproteobacteria* (52.6% in BF2 and 41.7% in AS2), *Clostridia* (5.6% in BF2 and 6.4% in AS2), *Anaerolineae* (5.3% in BF and 3.0% in AS), etc., were also predominant for both BF2 and AS2. However, the genera difference was found large for BF2 and AS2, and the denitrifying bacteria *Acinetobacter* (10.9%) and *Denitratisoma* (2.9%) were the predominant genera in BF2, while *Lactobacillus* (4.4%) and *Denitratisoma* (3.1%) were abundant in AS2. The PICRUSt prediction results illustrated that 33 predictive specific genes were related to denitrification process including NO_3^--N/NO_2^--N/NO/N_2O reductase and other denitrification-related genes. The relative abundance of 18 predictive specific genes in BF2 were higher than that in AS2, which indicated that the microorganisms in BF played more important role during denitrification.

Ethical statement

No conflict of interest exits in this manuscript. The work has not been published previously, and not under consideration for publication elsewhere. This article does not contain any studies with human participants and animals performed by any of the authors.

Acknowledgments

This work was supported by the National Major Science and Technology Program for Water Pollution Control and Treatment (Nos. 2017ZX07401003-05-01; 2014ZX07216-001) and the China Scholarship Council Foundation (No. 2011911098).

Appendix A. Supplementary data

Supplementary data to this article can be found online at https://doi.org/10.1016/j.jes.2019.04.030.

REFERENCES

Arantzazu, G.L., Ariadna, V.S., Rosalia, T., Sara, H., Lluís, B.E., 2011. Genetic potential for N_2O emissions from the sediment of a free water surface constructed wetland. Water Res. 45 (17), 5621–5632.

Bing, T., Yu, C., Bin, L., Zhao, Y., Feng, X., Huang, S., et al., 2016. Essential factors of an integrated moving bed biofilm reactor–membrane bioreactor: adhesion characteristics and microbial community of the biofilm. Bioresour. Technol. 211, 574–583.

Biswas, K., Taylor, M.W., Turner, S.J., 2014. Successional development of biofilms in moving bed biofilm reactor (MBBR) systems treating municipal wastewater. Appl. Microbiol. Biotechnol. 98 (3), 1429–1440.

Cao, X., Li, Y., Jiang, X., Zhou, P., Zhang, J., Zheng, Z., 2016. Treatment of artificial secondary effluent for effective nitrogen removal using a combination of corncob carbon source and bamboo charcoal filter. Int. Biodeterior. Biodegrad. 115, 164–170.

Chen, Y., Wen, Y., Cheng, J., Xue, C.H., Yang, D.H., Zhou, Q., 2011. Effects of dissolved oxygen on extracellular enzymes activities and transformation of carbon sources from plant biomass: implications for denitrification in constructed wetlands. Bioresour. Technol. 102, 2433–2440.

Christianson, L.E., Lepine, C., Sibrell, P.L., Penn, C., Summerfelt, S. T., 2017. Denitrifying woodchip bioreactor and phosphorus

filter pairing to minimize pollution swapping. Water Res. 121, 129–139.
Chu, L., Wang, J., 2016. Denitrification of groundwater using PHBV blends in packed bed reactors and the microbial diversity. Chemosphere. 155, 463–470.
Dong, Z., Lu, M., Huang, W., Xu, X., 2011. Treatment of oilfield wastewater in moving bed biofilm reactors using a novel suspended ceramic biocarrier. J. Hazard. Mater. 196 (1), 123–130.
Ge, S., Peng, Y., Wang, S., Lu, C., Cao, X., Zhu, Y., 2012. Nitrite accumulation under constant temperature in anoxic denitrification process: the effects of carbon sources and COD/NO_3-N. Bioresour. Technol. 114, 137–143.
Hang, Q., Wang, H., Chu, Z., Hou, Z., Zhou, Y., Li, C., 2017. Nitrate-rich agricultural runoff treatment by Vallisneria -sulfur based mixotrophic denitrification process. Sci. Total Environ. 587-588, 108–117.
Ji, Y., 2018. Opportunities and challenges to use electrical stimulation for enhanced denitrification in woodchip bioreactors. Ecol. Eng. 110, 38–47.
Kim, Y.M., Lee, D.S., Park, C., Park, D., Park, J.M., 2011. Effects of free cyanide on microbial communities and biological carbon and nitrogen removal performance in the industrial activated sludge process. Water Res. 45 (3), 1267–1279.
Kopec, L., Kopec, A., Drewnowski, J., 2018. The application of Monod equation to denitrification kinetics description in the moving bed biofilm reactor (MBBR). Int. J. Environ. Sci. Technol. (10–11), 1–8.
Langille, M.G.I., Zaneveld, J., Caporaso, J.G., Mcdonald, D., Knights, D., Reyes, J.A., et al., 2013. Predictive functional profiling of microbial communities using 16S rRNA marker gene sequences. Nat. Biotechnol. 31 (9), 814–821.
Li, X., Sun, S., Yuan, H., Badgley, B.D., He, Z., 2017. Mainstream upflow nitritation-anammox system with hybrid anaerobic pretreatment: long-term performance and microbial community dynamics. Water Res. 125, 298–308.
Liu, D., Li, J., Li, C., Deng, Y., Zhang, Z., Ye, Z., Zhu, S., 2018. Poly (butylene succinate)/bamboo powder blends as solid-phase carbon source and biofilm carrier for denitrifying biofilters treating wastewater from recirculating aquaculture system. Sci. Rep. 8 (1), 3289.
Matar, G.K., Bagchi, S., Zhang, K., Oerther, D.B., Saikaly, P.E., 2017. Membrane biofilm communities in full-scale membrane bioreactors are not randomly assembled and consist of a core microbiome. Water Res. 123, 124–133.
Noah, F., Jason, A.J., Rytas, V., Robert, B.J., 2005. Assessment of soil microbial community structure by use of taxon-specific quantitative PCR assays. Appl. Environ. Microbiol. 71 (7), 4117–4120.
Odegaard, H., Rusten, B., Westrum, T., 1994. A new moving bed biofilm reactor - applications and results. Water Sci. Technol. 29 (10), 157–165.
Pradhan, S., Fan, L., Roddick, F.A., Shahsavari, E., Ball, A.S., 2016. Impact of salinity on organic matter and nitrogen removal from a municipal wastewater RO concentrate using biologically activated carbon coupled with UV/H_2O_2. Water Res. 94, 103–110.
Satoshi, I., Naoaki, A., Shigeto, O., Keishi, S., 2011. Isolation of oligotrophic denitrifiers carrying previously uncharacterized functional gene sequences. Appl. Environ. Microbiol. 77 (1), 338–342.
Shannon, M.A., Bohn, P.W., Elimelech, M., Georgiadis, J.G., Mariñas, B.J., Mayes, A.M., 2008. Science and technology for water purification in the coming decades. Nature. 452 (7185), 301–310.
Shen, Z., Zhou, Y., Hu, J., Wang, J., 2013. Denitrification performance and microbial diversity in a packed-bed bioreactor using biodegradable polymer as carbon source and biofilm support. J. Hazard. Mater. 250–251 (8), 431–438.
Stres, B., Murovec, B., 2009. New primer combinations with comparable melting temperatures detecting highest numbers of nosZ sequences from sequence databases. Acta Argic Slov. 94 (2), 139–142.
Sun, H., Qiang, W., Ping, Y., Zhang, L., Lin, Y., Zhang, X.X., et al., 2017. Denitrification using excess activated sludge as carbon source: performance and the microbial community dynamics. Bioresour. Technol. 238, 624–632.
Torresi, E., Gülay, A., Polesel, F., Jensen, M.M., Christensson, M., Smets, B.F., et al., 2018. Reactor staging influences microbial community composition and diversity of denitrifying MBBRs - implications on pharmaceutical removal. Water Res. 138, 333–345.
Umar, M., Roddick, F.A., Fan, L., Autin, O., Jefferson, B., 2015. Treatment of municipal wastewater reverse osmosis concentrate using UVC-LED/H_2 O_2 with and without coagulation pretreatment. Chem. Eng. J. 260, 649–656.
Wei, Z., Ji, G., 2014. Quantitative response relationships between nitrogen transformation rates and nitrogen functional genes in a tidal flow constructed wetland under C/N ratio constraints. Water Res. 64 (7), 32–41.
Wouter, R.L.V.D.S., Wiebe, R.A., Dennis, B., Jan-Willem, M., Takaaki, T., Marc, S., et al., 2007. Startup of reactors for anoxic ammonium oxidation: experiences from the first full-scale anammox reactor in Rotterdam. Water Res. 41 (18), 4149–4163.
Xu, Z., Dai, X., Chai, X., 2018. Effect of different carbon sources on denitrification performance, microbial community structure and denitrification genes. Sci. Total Environ. 634, 195–204.
Yang, X.L., Jiang, Q., Song, H.L., Gu, T.T., Xia, M.Q., 2015. Selection and application of agricultural wastes as solid carbon sources and biofilm carriers in MBR. J. Hazard. Mater. 283, 186–192.
Yarullina, D.R., Ilinskaya, O.N., 2007. Genomic determinants of nitric oxide biosynthesis in *Lactobacillus plantarum*: potential opportunities and reality. Mol. Biol. 41 (5), 820–826.
Young, B., Banihashemi, B., Forrest, D., Kennedy, K., Stintzi, A., Delatolla, R., 2016. Meso and micro-scale response of post carbon removal nitrifying MBBR biofilm across carrier type and loading. Water Res. 91, 235–243.
Yuan, Q., Wang, H., Hang, Q., Deng, Y., Liu, K., Li, C., et al., 2015. Comparison of the MBBR denitrification carriers for advanced nitrogen removal of wastewater treatment plant effluent. Environ. Sci. Pollut. Res. 22 (18), 1–10.
Zhang, W., Wang, D., Jin, Y., 2017. Effects of inorganic carbon on the nitrous oxide emissions and microbial diversity of an anaerobic ammonia oxidation reactor. Bioresour. Technol. 250, 124–130.